Comparison between Two Types of Electrodes for Electrostatic Quadrupole Lens

Sura A. Obaid

Department of Physiology and Medical Physics, College of Medecine, Al-Nahrain University, Baghdad, Iraq.

E-mail: suraallawi@yahoo.com

Abstract

This work aims to find the optimum design of electrostatic quadrupole lens and make the comparison between two different electrodes shapes which are computed with the aid of transfer matrices. Two types of electrostatic quadrupole lens, cylindrical convex electrodes, and cylindrical concave electrodes were used to find optimum field model, which was close to the field distribution for each design of the proposed lens.

The path of charge-particles beam is traverse the field model has been determined by solving the trajectory equation of motion in Cartesian coordinates. Then, take the comparison of the optimum values of spherical aberration coefficients and resolution limits in both convergence and divergence plans for each proposed type.

Keywords: Electrostatic, quadrupole Lens, spherical aberration, resolution limits, trajectory equation.

الخلاصة

تهدف هذه الدراسة لايجاد التصميم الامثل لعدسة كهروستاتيكية رباعية الاقطاب مع اجراء مقارنة بين نوعين من هذه العدسات بالاستعانة بمفاهيم انتقال المصفوفات ، أحداهما ذات أقطاب اسطوانية بسطوح محدبة والاخرى ذات اقطاب اسطوانية بسطوح مقعرة لإيجاد أنموذج المجال الكهروستاتيكي الأمثل لكل تصميم من العدسات المفترضة أعلاه. يتم حساب مسار حزمة الجسيمات المشحونة المارة خلال أنموذج المجال بواسطة حل معادلة الحركة للأشعة بالإحداثيات الكارتيزيه، وقد تم مقارنة القيم المثلى لمعاملات الزيغ الكروي وحدود التحليل في كلا النموذجين المفترضين.

Introduction

Electron lenses are one of the principle components of the electron optics devices. Both electrostatic lens (electric field) and magnetic lens (magnetic field) are used to focuses charged particles; each type has its advantages and disadvantages. The focusing power of electrostatic lenses independent of the mass of the charged particles and depends only on their energy; therefore to be preferred over magnetic lenses when heavy particles of moderate energy must be focused.

There are numerous types of electrostatic lenses, each one of them classify according to electron-optical properties and domain of application. The first published work on electrostatic fields with rotational symmetry dates back to 1926 [1]. The quadrupole lenses are second in importance only to the axisymmetric electron lenses. Quadrupole lenses began to be used in electron-optical devices in the 1950 s. These lenses have a high focal power and are used to focus the beams in high-energy. They produce fields with two mutually perpendicular planes of symmetry and two planes of asymmetry by means of four identical electrodes arranged symmetrically about the axis. Therefore, if the x-z plane of the lens collects the charged particles, the y-z plane will cause them to diverge, i.e., the quadruple lens is astigmatic [2,3].

Lens Design

This work is concerned with the design of electrostatic quadrupole lens consist of four identical symmetric parts are cut out from cylinder. These four parts represent the concave and convex cylindrical quadrupole lens. The effect of changing the geometrical shape of electrodes for each design like; the angle of gape between electrodes (Γ), where the ratio of cylindrical electrode radius (R) to aperture radius (a) is constant, electrode voltage ratios (V/V_1), electrode thicknesses and spacing between them, as well as the radial and longitudinal dimensions of the electrode. The particular electrode configuration may be found in the value of (K) (electrode shape) and then the excitation parameter of lens as active parameter is changing [4,16].

Quadrupole lens is described as converging lens if the particles moving in x–z plane are deflected toward the z-axis and while described as diverging lens if the particles moving in y-z plane are deflected away from the z-axis [5]. In the current work, the electrodes shapes which taking into consideration are the cylindrical convex and cylindrical concave electrodes that generally used instead of hyperbolic electrodes due to the difficulties of fabricate.

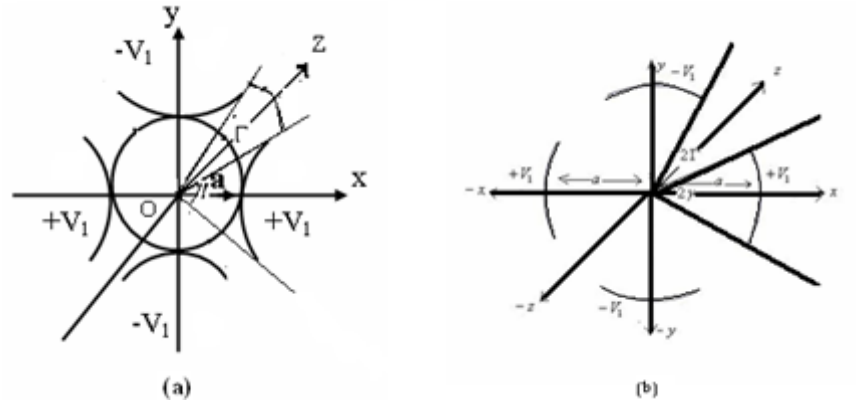

Figure 1. Electrodes of quadrupole lens: (a) cylindrical convex electrodes, (b) cylindrical concave electrodes [12,14].

The Potential Distribution

Variation of the parameter K according to electrode shape gives different modes of potential distribution. In cylindrical coordinates, the potential a long the optical axis is given by the formula;[4].

$$V(r,\theta,z) = D(z)\, V_1\, (r/a)^2 \cos(2\theta) \qquad (1)$$

where V_1 is the electrode potential (take 100 volt in the current study), r is the of the radial displacement of the beam from the optical axis measured in (mm), θ is the angle between electrodes and z-axis measured in degree, and D(z) is the electrodes field (the quadrupole field components) which is equal to; [6].

$$D(z) = K\ f(z) \qquad (2)$$

Thus, $f(z)$ refers to function mode which is normalized to unity at the center $z = 0$.

The parameter K (K1,K2) named the electrode shape, determined by the electrode geometry from K1 and K2 which is represented the coefficients of the electrode shape for cylindrical convex (K1) and cylindrical concave electrodes (K2) respectively are described as equations; [4,6]

$$K1 = 2\sin(\Gamma) / \ln(R/a) \qquad (3)$$

$$K2 = 4\sin(\Gamma) / \pi \qquad (4)$$

Where R is the radius of cylindrical convex electrode equal to [4]

$$R = 1.2\ a \qquad (5)$$

The effective lengths of the electrodes L_1 for convex electrodes, L_2 for concave electrodes are given by relations [1].

$$L_1 = \ell + 0.1056\, a \qquad (6)$$

$$L_2 = \ell + 0.451\, a \qquad (7)$$

Where ℓ is geometrical length of electrodes.

The Trajectory of Electron Beam

In the present work the polarities of each electrode of the x and y axes as shown in figure (1). Since the positive potential (+V_1) is applied on the x–axis electrodes of the lens, then the positively charged particles will be repelled along the x–axis and will be directed towards the z–axis. The positively charged particles will be attracted by the negative potential (–V_1) along the y–axis of the lens.

The trajectory equations in cartesian coordinates for the charged particles beam traversing the field of a quadrupole lens are given by [3]:

$$x'' + \beta^2 f(z)x = 0 \qquad (8)$$

$$y'' - \beta^2 f(z)y = 0 \qquad (9)$$

Where β is the excitation parameter given by the following relation [3].

$$\beta^2 = V_1 K / a^2 V_0 \qquad (10)$$

Where V_0 acceleration voltage, x'' and y'' are the second derivatives with respect to z [7,8].

Where $f(z)$ is the modified bell–shaped field model as in figure (2) represents the intermediate case between the rectangular section of constant maximum value $f(z)_{max} = 1$ in the region $-z_L \le z \le z_L$ and beyond these boundaries it terminates in the form of a half bell - shaped field represented by the following function [3].

$$f(z) = 1/[1+((z-z_L)/d)^2]^2 \text{ when } z > z_L \qquad (11)$$

$$f(z) = 1/[1+((z+z_L)/d)^2]^2 \text{ when } z < -z_L \qquad (12)$$

Where d is the axial extension of the field between the two points.

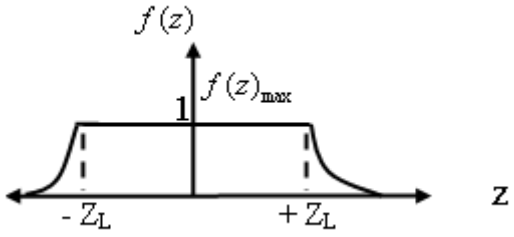

Figure 2. Field distribution of a quadrupole lens (Modified bell–shaped model) [15].

The Spherical aberration

The Spherical aberration is the name given to the effect where the focal length of a lens will vary depending on how far you are from the centre of the lens. What this means in reality is that a parallel rays of light entering the lens near its centre, will be focused less or more than a parallel ray entering near the edges of the lens. In a quadrupole lens, the spherical aberration in

the gaussian image plane can be expressed as [3,9] and [14].

$$\Delta x(zi) = M_x\ (C_s\ \alpha^3 + C_p\ \alpha\ \delta^2) \quad (13)$$

$$\Delta y\ (zi) = M_y\ (D_p\ \alpha^2\ \delta + D_s\ \delta^3) \quad (14)$$

Where α and δ are the image side semi–aperture angles in the x–z and y–z plane, respectively. The coefficients C and D characterize the aberration in the convergence and divergence plane, retrospectively. The coefficient C_s determines the aberration of the real width image in the plane y = 0, and D_s is that for the imaginary image in the plane of x = 0 [10].

The spherical aberration coefficients C and D are given by the forms [7].

$$C_s = \frac{d}{32\sin^4\psi_0}[(w_x^2-1)(w_x^2+3)\frac{\pi}{w_x^5} + \frac{2(7-w_x^2)}{4w_x^2-1}(\sin 2\psi_0 - \sin 2\psi_1) + (2-2n+3n^2)$$
$$(w_x^2-1)[(w_x^2-1)\frac{\pi}{w_x^5} - \frac{2}{4w_x^2-1}(\sin 2\psi_0 - \sin 2\psi_1)]] \quad (15)$$

And [7].

$$C_p = \frac{d}{32\,w_y^2\sin^4(\psi_0)}[[-4[(1-\cos(2\pi\frac{w_y}{w_x}))\ \sin(2\psi)_1 + w_y(1-\cos(2\psi_1)\ \sin(2\pi\frac{w_y}{w_x})]$$
$$+3(w_x^2-1)[-2(w_x^2-1)\frac{\pi}{w_x^3} + \frac{1}{w_x^2-1}[-\frac{w_y{}^2(w_x^2w_y^2+2)}{4w_x^2\,w_y^2-1}\sin(2\psi_0) + (w_y^2+3)$$
$$\sin(2\psi_1) + \frac{3w_y^2+1}{2w_y}\sin(2k\pi\frac{w_y}{w_x})] - \frac{3}{4w_x^2w_y^2-1}[(4w_y^2-1)\sin(2\psi_1)\cos(2\pi\frac{w_y}{w_x}) \quad (16)$$
$$+w_y(2w_y^2+1)\cos(2\psi_1)\ \sin(2\pi\frac{w_y}{w_x})]] + (2+2n-n^2)\ (w_x^2-1)[2(w_x^2-1)\frac{\pi}{w_x^3} -$$
$$\frac{4w_y^2(w_x^2-1)}{4w_x^2w_y^2-1}\sin(2\psi_0) + \sin(2\psi_1) - \frac{1}{2w_y}\sin(2\pi\frac{w_y}{w_x}) - \frac{1}{4w_x^2\,w_y^2-1}[(4w_y^2-1)$$
$$\sin(2\psi_1)\ \cos(2\pi\frac{w_y}{w_x}) + w_y(2w_y^2+1)\cos(2\psi_1)\sin(2\pi\frac{w_y}{w_x})]]]]$$

$$D_s = \frac{d(w_x^2-1)}{32\,w_y^4 \sin^4(\psi_0)}[-\frac{1}{3}[2\ (2+n)\,w_y\,(1-\cos(2\psi_1))\ (1-\cos(2\pi\frac{w_y}{w_x}))\ \sin(2\pi\frac{w_y}{w_x})$$
$$+(4-n)(\cos(4\pi\frac{w_y}{w_x})-4\cos(2\pi\frac{w_y}{w_x})+3)\ \sin 2\psi_1]-(w_y^2+3)\frac{\pi}{w_x}+$$
$$\frac{2w_y^4(5+w_x^2)}{(w_x^2-1)(4w_y^2-1)}\sin(2\psi_0)+\frac{1+w_x^2}{2}\sin(2\psi_1)+\frac{2}{w_y}\sin(2\pi\frac{w_y}{w_x})-\frac{w_x^2-1}{4w_y}$$
$$\sin(4\pi\frac{w_y}{w_x})-\frac{2}{w_x^2-1}[(w_y^2+1)\sin(2\psi_1)\cos(2\pi\frac{w_y}{w_x})+2w_y(\cos 2\psi_1)$$
$$\sin(2\pi\frac{w_y}{w_x})]-\frac{1}{2(4w_y^2-1)}[(5w_y^2+1)\sin(2\psi_1)\cos(4\pi\frac{w_y}{w_x})+2w_y(w_y^2+2)$$
$$\cos(2\psi_1)\sin(4\pi\frac{w_y}{w_x})]+\frac{1}{3}(2-2n+3n^2)\ (w_x^2-1)\ [\frac{3\pi}{w_x}+\frac{6w_y{}^4}{(w_x^2-1)(4w_y^2-1)}$$
$$\sin(2\psi_0)+\frac{2}{3}\sin(2\psi_1)-\frac{2}{w_y}\sin(2\pi\frac{w_y}{w_x})+\frac{1}{4w_y}\sin(4\pi\frac{w_y}{w_x})-\frac{2}{w_x^2-1}(\sin(2\psi_1)$$
$$\cos(2\pi\frac{w_y}{w_x})+w_y\cos(2\psi_1)\sin(2\pi\frac{w_y}{w_x}))-\frac{1}{2(4w_y^2-1)}(\sin(2\psi_1)\cos(4\pi\frac{w_y}{w_x}) \qquad (17)$$
$$+2w_y\cos(2\psi_1)\sin(4\pi\frac{w_y}{w_x})]]$$

Also [7].

$$D_P = C_P - \frac{d}{8\,w_y^2\sin^4(\psi_0)}[(1-\cos(2\pi\frac{w_y}{w_x}))\sin(2\psi_1)+w_y\ (1-\cos(2\psi_1)) \qquad (18)$$
$$\sin 2\pi\frac{w_y}{w_x}]$$

Where ψ_0 is the value corresponds to the position of the object and ψ_1 to that of the image, and $(n=-1)$ for electrostatic quadrupole lens.The properties of the quadrupole lens are characterized by the parameter [7].

$W_x = 1-\beta^2 d^2$ for the convergence plane (19)

$W_y = 1+\beta^2 d^2$ for the divergence plane (20).

The Limiting Resolution

The resolving power of any optical device is the ability to form two separate images of two point objects very close together. The theoretical limit of resolution of microscope is determined by the combined effect of chromatic and spherical aberrations. The practical resolution of any instrument also depends on the supplementary aberrations that arise from constructional defects, or the observer himself, or from mechanism of interaction between the beam

and the object to be observed. The resolution limit is given by equation [11].

$$R = 0.61\,(C\,\lambda^3)^{1/4} \qquad (21)$$

Where λ is the electron wavelength which is given by the form[11].

$$\lambda = \sqrt{\frac{1.5}{V_0}} \qquad (22)$$

Results and Discussion

The axial potential distribution ratio $(V(\theta)/V_1)$ represented in equation (1) is plotted as a function of theta, as shown in figure (3) ,it is found that very close to modified bell-shaped model by use quadrupole lenses of cylindrical convex and cylindrical concave electrodes. This result agrees with the results mentioned in various references such as [6,12,13], and [14].

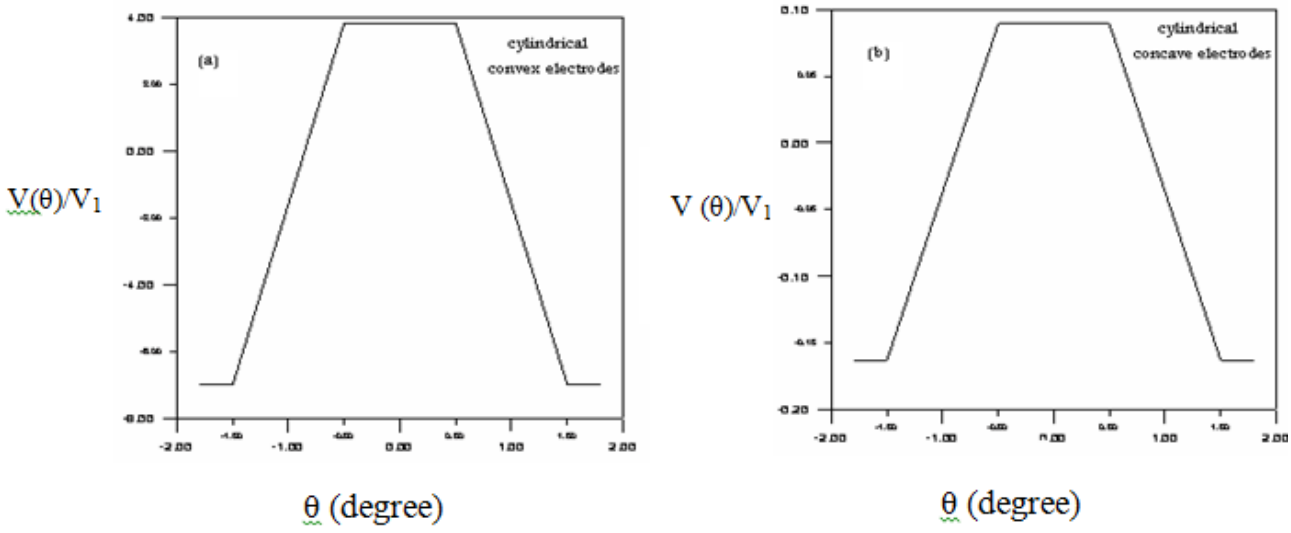

Figure 3. The axial potential distribution ratio $(V(\theta)/V_1)$ as a function of θ for electrostatic quadrupole lens with cylindrical (a)convex and (b) concave electrodes.

The values of K and β computed from equations (3), (4), and (10) are represented as a function of Γ as shown below in figure (4) which is illustrate in the increment in Γ leads to firstly increasing in K and β arriving to maximum values of K_1 =1.097 and $\beta_1 = 0.11$ mm^{-1} at $\Gamma = 45.55^\circ$ for concave electrodes and has the same behavior in convex electrodes with K_2 =1.273 and $\beta_2 = 0.038$ mm^{-1} at $\Gamma = 45.55^\circ$. Then drop to low values (decreases). The excellent agreement shown with other literatures Baranova and Yavor in [1].

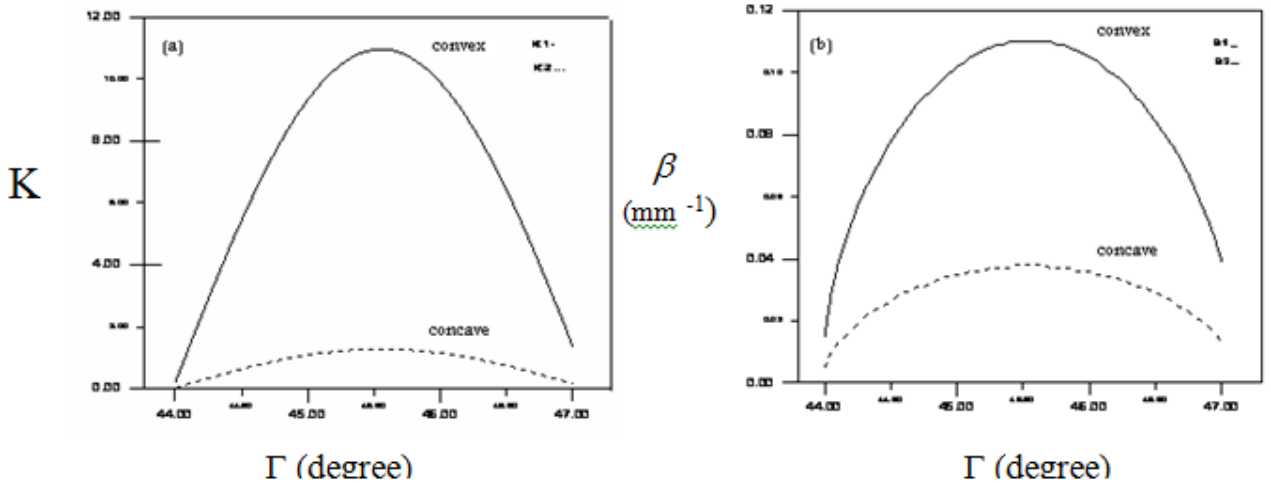

Figure 4. (a) The coefficient of electrode shape K , (b) the excitation parameter β as a function of gap angle Γ.

The trajectory equation of charge particles has been solved for the case of modified bell-shaped model by using simplified transformation for equations (8) and (9). When $\beta_1 = 0.11 mm^{-1}$, $\beta_2 = 0.038\ mm^{-1}$, and z = 5-20 mm in case modified bell-shaped model. These equations describe the paths of charge particles in convergence and divergence plane respectively. In electrostatic quadrupole lens charge particles incident in the (x-z) plane different paths from that in the (y-z) plane, as shown in figure (5). From figure (5) shows the charge particles in the convergence plane (x-z plane) is deflected toward the optical axis (z), while in the divergence plane (y-z plane) is away from the optical axis. i.e. the quadrupole lens is astigmatic, and the results is identify with that published by Baranova and Yavor in [1].

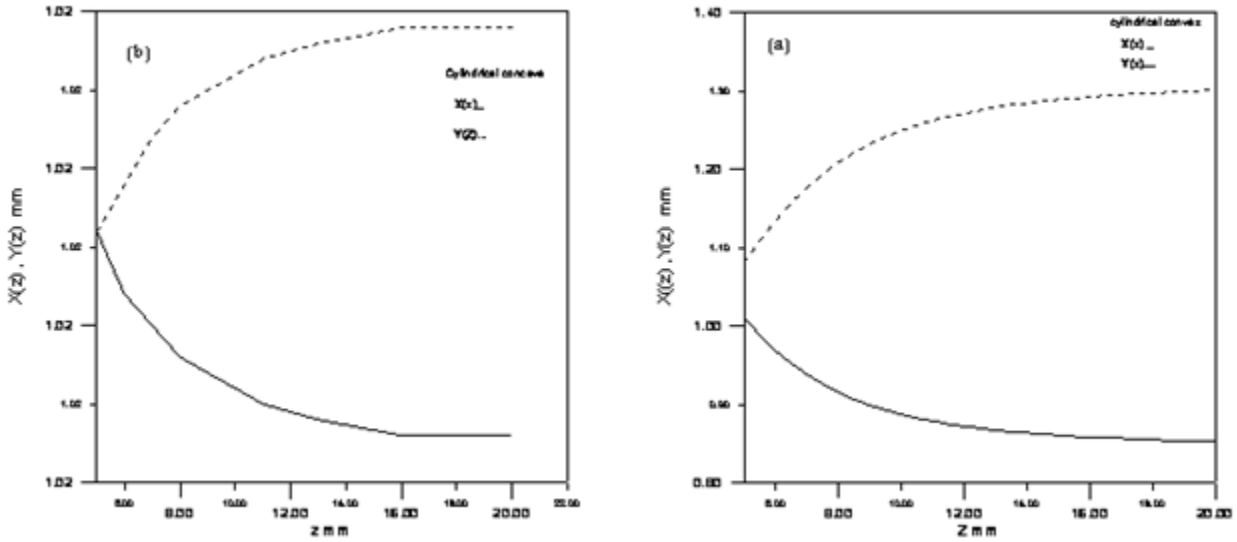

Figure 5. Trajectory of charge particles in electrostatic quadrupole lens with cylindrical (a) convex and(b) concave electrodes for both convergence (x−z) plane and divergence (y−z) plane.

The estimation of optimization for spherical aberration coefficients in both convergence and divergence plane improved the effects of changing the electrode angle and the electrode shape of these lenses on the objective properties (spherical aberration coefficients), as shown in figures 6 and 7, for convergence and divergence plane, respectively.

Figure 6 shows the proportionally relation between spherical aberration coefficient C_{p1}, C_{p2} ,C_{s1},C_{s2} , and Γ for the convergence plane in two electrode shapes, where the spherical aberration coefficient C_{p1} for the electrostatic quadrupole lens of cylindrical convex electrodes and C_{p2} the electrostatic quadrupole lens of cylindrical concave electrodes are decreasing in negative value as Γ is increasing and they have a minimum values $C_{p1} = -69.156$ and $C_{p2} = -14.284$ at $\Gamma = 45.55^{\circ}$.

The lowest absolute value of spherical aberration coefficients C_{p1},and C_{p2} are found after and before these minimum values.

The spherical aberration coefficients C_{s1}, and C_{s2} have the same behavior in all rang of gap angle Γ and the lowest absolute accurate values of these coefficients should be at range $44.5^{\circ} \le \Gamma \le 46.5^{\circ}$. The minimum absolute values of C_{s1} = 4.885 and C_{s2} = 1.885 at $\Gamma = 45.55^{\circ}$.

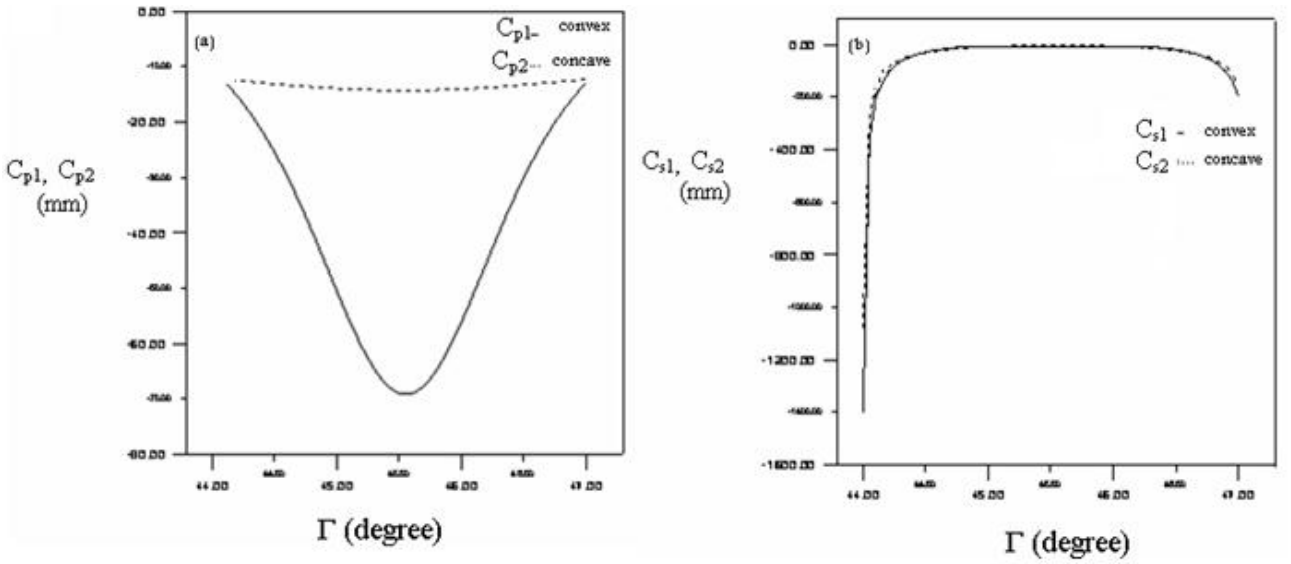

Figure 6. The spherical aberration coefficients (a) C_{p1} and C_{p2}, (b) C_{s1} and C_{s2} as a function of gap angle Γ.

The spherical aberration coefficients D_{p1} and D_{p2} in divergence plane represented as a function of Γ as shown in figure 7-a. According to figure 7-a we notice the values of D_{p1} are always positive and increasing with Γ up to maximum value (13.11) mm at Γ = 45° then happen slow drop then up to the same maximum value at Γ = 46.1°. Therefore drop sharply with increasing Γ. While, the values of D_{p2} are always negative and decreases in its absolute values with increment of Γ until (7.16) mm at Γ= 45.5°.then dropping with increasing Γ.

The last parameter of spherical aberration coefficients are D_{s1} and D_{s2} represented as a function of Γ shown in figure 7-b, which has the same behavior for all values of Γ. The values of D_{s1} and D_{s2} are always negative, and these values increases with Γ increases. These parameters be have as constant values at $\Gamma \geq 44.5^{\circ}$. The D_{s1} give us the better absolute value than D_{s2} which is 1.12 mm at Γ =45.55°.

One can be concluded from figures (6) and (7) that the variation of the four spherical aberration coefficients as a function of Γ, give us the best values for the cylindrical convex electrodes for whole range of Γ.

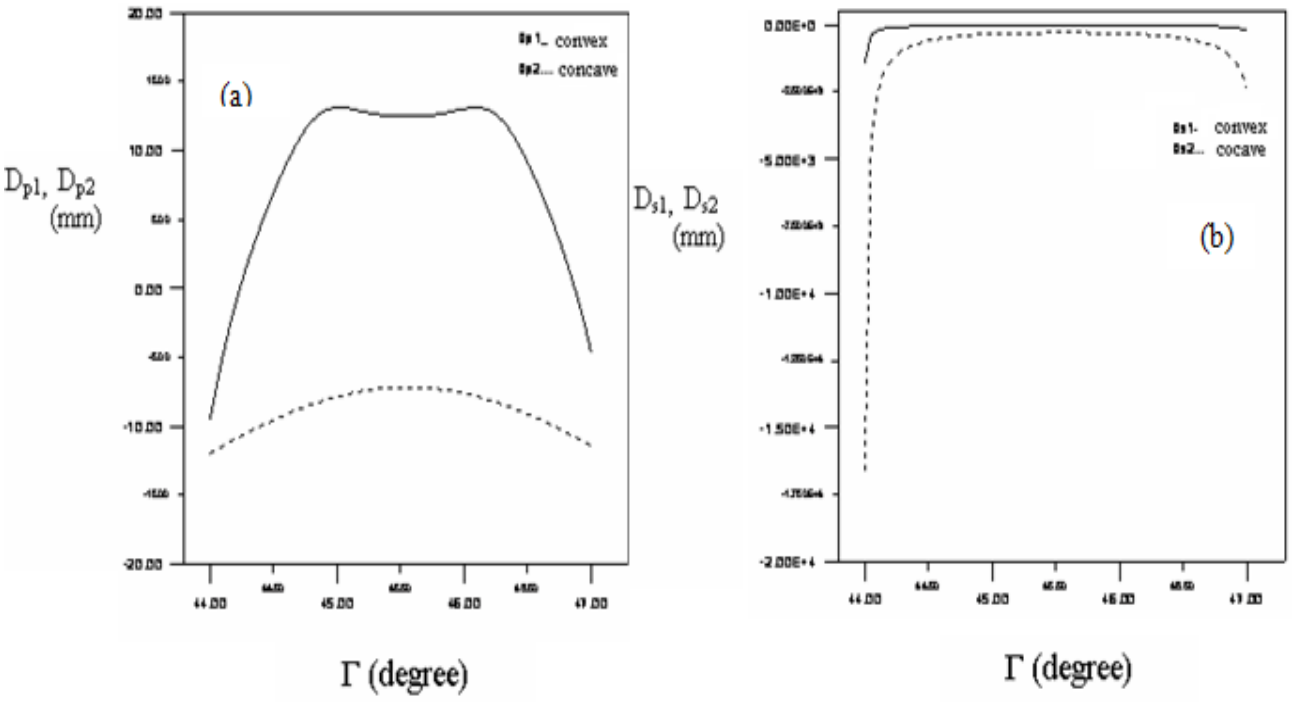

Figure 7. The spherical aberration coefficients of electrostatic quadrupole lens (a) D_{p1}, D_{p2}, and (b) D_{s1}, Ds2 as a function of gap angle Γ.

The resolution limit computes according to equation (21) and (22). Representing the resolution limits R_{cs1} and R_{cs2} as a function of Γ shown in figure (8-a), which has the same curve behavior with minimum values $R_{cs1} = 0.001$ nm at $\Gamma = 45.15^{\circ}$, and $R_{cs2} = 0.0029$ nm at $\Gamma = 45.55^{\circ}$.

While, the resolution limits R_{cp1} and R_{cp2} represented as a function of Γ shown in figure (8-b). The values of R_{cp1} increasing with increment Γ up to maximum values $R_{cp1} = 0.002$ nm, and the values of R_{cp1} increasing slowly with increasing Γ up to maximum values $R_{cp2} = 0.002$ nm, these maximum values happen at $\Gamma = 45.55$ and then drop with increasing Γ.

Representing the resolution limits R_{Ds1} and R_{Ds2} as a function of Γ shown in figure (9-a), which has approximately the same behavior with minimum values $R_{Ds1} = 0.00073$ nm, and $R_{Ds2} = 0.00292$ nm at $\Gamma = 45.55^{\circ}$. While the resolution limits R_{Dp1} and R_{Dp2} represented as a function of Γ shown in figure (9-b). The values of R_{Dp1} increasing with increment Γ up to maximum values $R_{Dp1} = 0.0013$ nm at $\Gamma = 45.05^{\circ}$, then happen slow drop and up to the same maximum value at $\Gamma = 46.05^{\circ}$, therefore, drop sharply with increasing Γ. Thus, the values of $R_{Dp}2$ decreasing with increasing of Γ until minimum values $R_{Dp2} = 0.01162$ nm at $\Gamma = 45.55^{\circ}$, then increasing these values with increasing Γ.

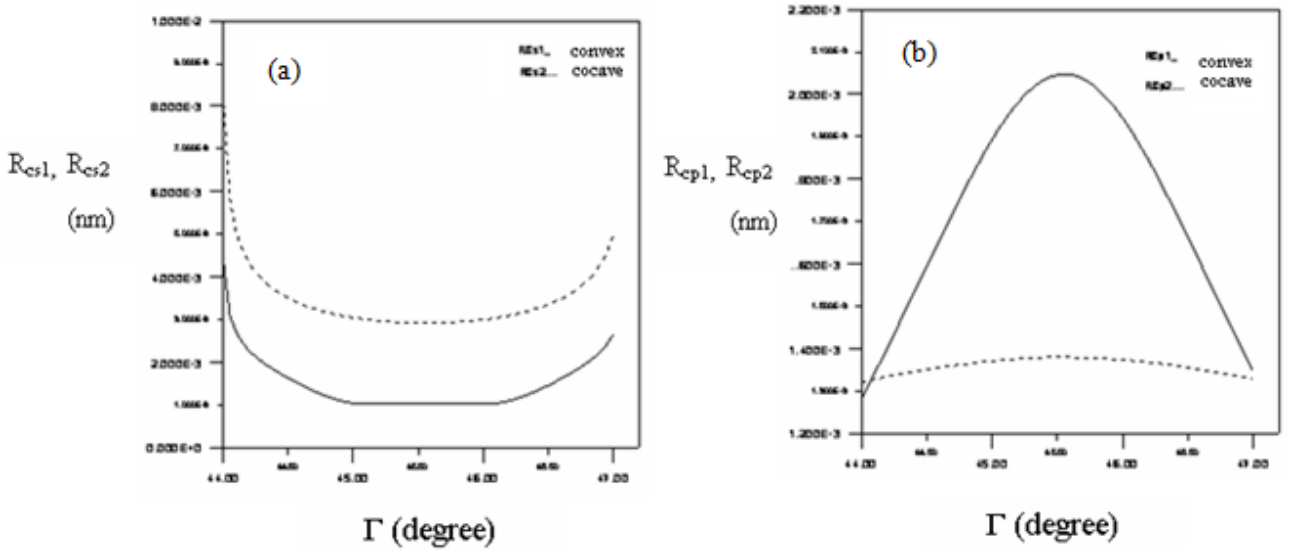

Figure 8. The resolution limit of electrostatic quadrupole lens (a) R_{cs1}, R_{cs2}, and (b) R_{cp1}, R_{cp2} as a function of gap angle Γ.

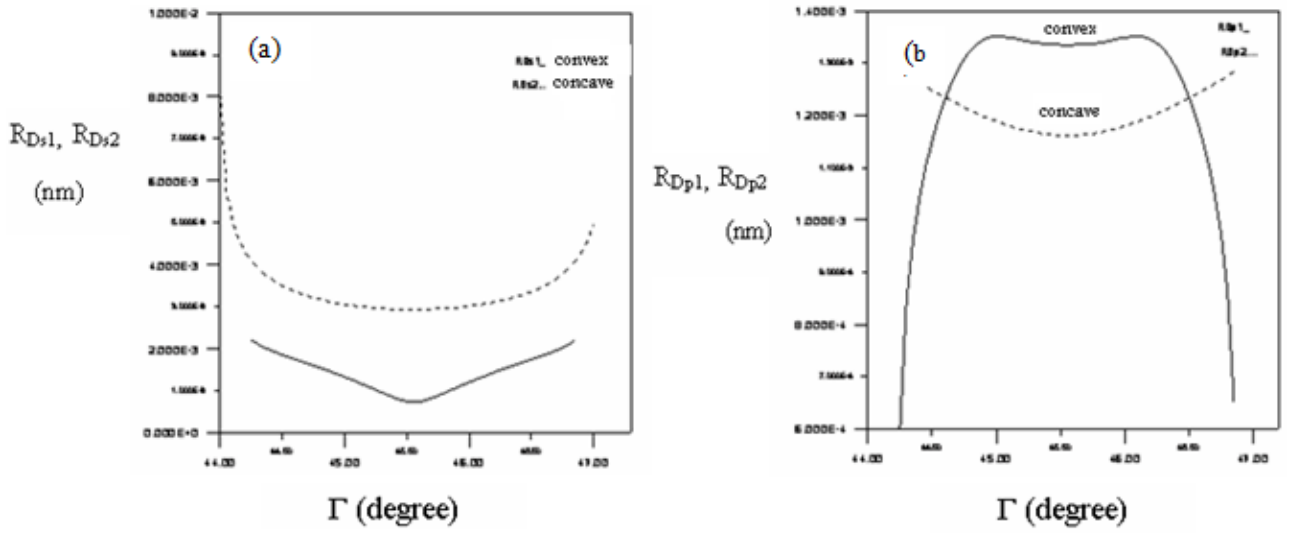

Figure 9. The resolution limit of electrostatic quadrupole lens (a)R_{Ds1}, R_{Ds2}, and (b) R_{Dp1}, R_{Dp2} as a function of gap angle Γ.

Conclusions

The quadrupole lens system has many variable geometrical and operational parameters; thus conclusive result is rather difficult. However, from the present investigation one may conclude the following:

a. It appears that the modified bell-shaped field model very close to the axial field distribution of the electrostatic quadrupole lens of concave and convex electrodes and it gives good properties.

b. In general, the electrostatic quadrupole lens of concave electrodes gives the best result of all spherical aberration parameters and resolution limit (or resolving power) than the electrostatic quadrupole lens of cylindrical convex electrodes.

References

1. Baranova, L. A. and Yavor, S.Ya. (1984), Electrostatic lenses, Sov.Phys.Tech.Phys., **29** (8),827-847.

2. S.Ya. Yavor, (1968) ,p.263 "Focusing of charged particles by Quadruple lenses ".

3. P.W. Hawkes, (1970), "Quadrupoles in electron lens design", Adv.Electronics and Electron Phys.Supplement 7, ed. L. Marton, (Academic Press, New York and London).

4. M. Szilagyi, (1988),"Electron and ion optics", (Plenum Press, New York).

5. Grime, G.W. and Watt, F. (1988),"Focusing protons and light ions to micron and submicron dimensions "Nuclear Instruments and Methods in Physics Research, B30, 227-234.

6. A. Kiss and E. Koltay, (1970),"Investigations on the effective length of asymmetrized quadrupole lenses", Nucl.Instrum. Meth.78, 238-244.

7. A. D. Dymnikov, T. Ya. Fishkova and S.Ya. Yavor, (1965), "Spherical aberration of compound quadrupole lenses and systems ", Nucl. Instrum. Meth., 37, 268-275.

8. P. Grivet, (1972),"Electron Optics", (Pergamon Press, Oxford and New York).

9. Okayama, S. (1989), "Electron beam lithography using a new quadrupole triplet", SPIE, Electron-beam, X-ray, and Ion-beam Tectnology: Submicrometer Lithographies VIII, **1089**, PP 74-83.

10. Fishkova, T. Ya., Baranova, L. A., and Yavor, S. Ya. (1968), "Spherical aberration of stigmatic doublet of quadrupole lenses" (rectangular model).Sov.Phys.Tech.Phys.,13 (4),520-525.

11. P.W. Hawkes, (1972), " Electron optics and electron microscopy", Taylor & Francis LTD, (10-14 Macklin Street London WC2B5NF).

12. T. Hayashi and N. Sakudo, (1968), " Quadrupole field in circular concave electrodes ", Rev. Sci. Instrum., 39 (7),958-961.

13. S. Okayama and H. Kawakatsu, (1978), "Potential distribution and focal properties of electrostatic quadrupole lenses", J. Phys.E: Sci. Instrum., 11, 211-216.

14. Oday A. Hussein, (2009), "Determination of the most favorable shapes for the electrostatic Quadrupole " , J. Al-Nahrain University, Science , 12 (3), 86-93.

15. Hawkes, P.W. (1965/1966), "The electron optics of a quadrupole lens with triangular potential", Optik, 23, 145-168.

16. L.R. Burns et al. (2007), "Evaluation of a novel design for an electrostatic quadrupole triplet ion beam lens", Nucl. Instr. and Meth. B.04.215